Influence of the diffusive boundary layer on solute dynamics in the sediments of a seiche-driven lake: A model study

Andreas Brand,[1] Christian Dinkel,[2] and Bernhard Wehrli[2,3]

Received 14 April 2008; revised 29 September 2008; accepted 18 November 2008; published 17 February 2009.

[1] The diffusive boundary layer (DBL) plays an important role in the transport of electron acceptors for mineralization and oxidation processes in highly reactive sediments. We used transient numerical modeling to characterize the effects of the DBL thickness on solute dynamics in the sediments of Lake Alpnach. Our model study shows that the DBL mainly influences short-term sedimentary denitrification by resisting transport. The DBL also governs the reoxidation of reduced compounds by controlling the oxygen penetration depth in the sediment. An increase of the DBL thickness from 0.25 to 1.5 mm diminished the oxygen flux into the sediment by more than 30% from 15 to 9.5 mmol m^{-2} d^{-1}. At the same time, this change in DBL thickness had contrasting effects on the reoxidation of reduced solutes released in the anoxic sediment layers: While the rates of Fe(II) and Mn(II) oxidation decreased by up to 60%, the oxidation of methane changed by only 2%. Still, the contribution to the total oxygen uptake by these redox processes never exceeded 40%. Denitrification rates under steady state conditions were only 8% slower when the DBL was extended from 0.25 to 1.5 mm. The decreased nitrate supply was partially compensated by a stimulated denitrification process due to the lower oxygen penetration. However, fluxes of nitrogen species periodically deviated by more than 60% when an oscillating DBL thickness with periods of less than 6 h was modeled.

Citation: Brand, A., C. Dinkel, and B. Wehrli (2009), Influence of the diffusive boundary layer on solute dynamics in the sediments of a seiche-driven lake: A model study, *J. Geophys. Res.*, *114*, G01010, doi:10.1029/2008JG000755.

1. Introduction

[2] The importance of the diffusive boundary layer (DBL) for sediment oxygen dynamics is commonly known [e.g., *Boudreau and Guinasso*, 1982, *Jørgensen and Revsbech*, 1985]. The dynamic effects of a variable DBL thickness were included only recently in numerical models of early diagenesis. Such detailed reaction-transport models allowed quantifying the physical effects of the DBL structure on the mineralization and reoxidation processes in marine systems [*Glud et al.*, 2007; *Kelly-Gerreyn et al.*, 2005].

[3] The DBL is the region immediately above the sediment water interface (SWI) where turbulence is dampened and molecular diffusion becomes the dominant solute transport mechanism across the SWI [*Boudreau and Guinasso*, 1982]. Since molecular diffusion is generally orders of magnitude slower than turbulent or advective transport, the DBL mainly acts as a bottleneck between the open waters and the sediment. Fluxes across the DBL are mainly governed by molecular diffusion, the thickness of the DBL and the concentration gradient across the DBL.

[4] *Jørgensen and Revsbech* [1985] used oxygen microelectrodes to analyze the structure of the DBL in laboratory flumes. They found that the DBL can limit the oxygen uptake rate in sediments with highly reactive reduced compounds. The thickness of the DBL varies with sediment topography and bulk flow velocity [*Gundersen and Jørgensen*, 1990; *Jørgensen and Marais*, 1990; *Røy et al.*, 2002]. The first in situ investigations of the structure of the DBL were performed using indirect methods. *Santschi et al.* [1983] estimated the DBL thickness by recording the mass loss of gypsum plates laid out at the ocean floor. Early direct in situ measurements of the DBL using oxygen electrodes were reported for the Santa Catalania Basin in 1989 [*Archer et al.*, 1989]. *Steinberger and Hondzo* [1999] investigated the velocity dependence of the DBL thickness δ_{DBL} in the laboratory under steady state conditions and found that it increases with decreasing shear velocity following the scaling relation $\delta_{DBL} \sim u_*^{-1}$, where u* is the shear velocity. Recent studies showed that the DBL is also highly dynamic at short time scales. *Røy et al.* [2004] observed that fluctuations of oxygen concentrations in the DBL can also penetrate into the sediment. *Hondzo et al.* [2005] showed that the mass transfer is not limited to molecular diffusion. Oxygen can also be transferred to the sediment by sweep and eject motions which periodically replace the water at the sediment water interface [*O'Connor and Hondzo*, 2008a].

[1]Department of Civil and Environmental Engineering, University of California, Berkeley, California, USA.
[2]Surface Waters Research and Management, Eawag, Kastanienbaum, Switzerland.
[3]Institute of Biogeochemistry and Pollutant Dynamics, ETH Zurich, Zurich, Switzerland.

Copyright 2009 by the American Geophysical Union.
0148-0227/09/2008JG000755

[5] The first in situ investigation of the response of the DBL thickness on variable flow velocity near lake sediments was performed in seiche-driven prealpine Lake Alpnach [*Lorke et al.*, 2003]. The DBL thickness varied between 0.16 and 0.84 mm during one seiching period. *Lorke et al.* [2003] observed a time lag of 1.5 h between the thickness of the DBL and the measured current. The same time lag was observed between the current and the dissipation rate ε of the turbulent kinetic energy [*Lorke et al.*, 2002]. Therefore, the thickness of the DBL depends on the present turbulence rather than on the current flow shear in low-energetic, periodically sheared systems like Lake Alpnach. In these systems, the thickness of the DBL is described very well by the Batchelor length scale

$$L_B = 2\pi\left(\frac{\nu D^2}{\varepsilon}\right)^{1/4}, \quad (1)$$

where ε is the dissipation rate of turbulent kinetic energy, D is the molecular diffusion coefficient, and ν is the kinematic viscosity.

[6] The extent of the influence of the DBL on the dynamics of oxygen and other solutes in the sediment depends on the nature of the prevailing reactions in the sediment. *Jørgensen and Boudreau* [2001] illustrated the potential influence of the DBL on the oxygen flux into the sediment by discussing the analytical solutions for two extreme cases. First, in reactive sediments, the DBL can influence the consumption of oxygen where mineralization of organic matter acts as the primary oxygen sink. Second, the oxygen flux is completely independent of the DBL thickness, if oxygen is used only for the instantaneous oxidation of dissolved reduced compounds (RC) like sulfide. A change in the penetration depth of oxygen into the sediment is observed in both cases. These findings were confirmed recently in more detailed numerical studies. *Glud et al.* [2007] used a dynamic model to show that the DBL has only a minor influence on the oxygen flux at Aarhus Bay where oxygen is mainly consumed by secondary reactions like ammonia and manganese oxidation. In contrast, *Kelly-Gerreyn et al.* [2005] found that fluxes of oxygen, nitrate and sulfate can vary substantially with changing DBL thickness. In their model, they assumed that oxygen was only used by organic matter mineralization and ammonium oxidation. Highly reactive particulate organic matter showed more sensitivity to changing DBL than refractory material. Both studies were conducted in marine environments.

[7] Variations of the DBL should affect the denitrification process in a similar way as oxygen consumption, since nitrate is the most energy efficient electron acceptor after oxygen. Such an effect has been suggested by *Höhener and Gächter* [1994], who found that the sedimentary nitrate flux and ammonium release determined from benthic chambers correlated well with the stirring velocity of the water.

[8] *Baumann et al.* [1997] investigated the dynamic behavior of denitrification under variable conditions. They studied the response of both pure cultures like *Paracoccus denitrificans* and mixed cultures under alternating aerobic-anaerobic conditions in batch experiments and found that the efficiency of N_2 production and the composition of the intermediates depended highly on the duration of the time intervals. When the anaerobic period was 24 h, the cultures reached stable denitrification activities and N_2 was the only denitrification product released. If the duration of the anaerobic periods was short, a semi steady state was reached after several cycles and nitrite accumulated as the dominant denitrification product. Such changes in reaction pathways were expected on the basis of earlier kinetic modeling of *Wild et al.* [1995]. They showed that differences in denitrification rates and products under varying oxygen conditions could be explained by including the oxygen-dependent formation and degradation of denitrifying enzymes. Temporal variability in oxygen flux due to changes in the DBL thickness has the potential to induce similar responses in sediments, with implications for denitrification rates.

[9] Recent studies on denitrification dynamics under variable flow velocities in the overlying waters revealed a complex interplay between solute transport through the sediment water interface and the resulting response of microbes. *O'Connor and Hondzo* [2008b] observed an increased NO_3^- loss with increasing flow velocity as long as the shear velocity was below 0.23 cm s^{-1}. At high fluid flow, increasing velocity inhibited denitrification, since the increasing oxygen penetration depth restricts denitrification to a zone with lower denitrification potential. Similar observations were reported by *Arnon et al.* [2007]: changing hydrodynamic conditions caused facultative bacteria to shift between aerobic and anaerobic metabolism.

[10] In this paper we focus on the effects of seiche-induced variability of oxygen concentration and DBL thickness on mineralization and reoxidation processes in mesotrophic Lake Alpnach (Switzerland). We measured high-resolution oxygen and nitrate concentration profiles in the uppermost sediment in combination with concentration profiles of manganese, methane and iron in order to estimate the kinetic parameters for oxygen consumption and denitrification. A series of diffusion-reaction models with increasing complexity were implemented and analyzed in order to answer the following questions:

[11] (1) To which extend do oxygen fluxes respond to a variable DBL thickness? (2) How important are the fluxes of reduced compounds for O_2 consumption and how sensitively do these fluxes respond to changes in the DBL thickness? (3) How does seiching influence oxygen and denitrification dynamics? Will average flux values change with the frequency of these oscillations?

2. Study Site and Measurements

2.1. Study Site

[12] Oxygen and nitrate microprofiles were recorded on the southeast slope of Lake Alpnach (46° 57′ 51″ N, 8° 18′ 13″ E) on 14 and 15 September 2005 at a depth of 27 m. Velocity and temperature was monitored throughout the campaign at the same location. The lake is a medium-sized mesotrophic subbasin of Lake Lucerne in central Switzerland. Lake Alpnach has an elliptical shape of approximately 5 by 1.5 km, a surface area of 4.2 km^2, and a maximum depth of 34 m [*Gloor et al.*, 1994], and is separated by a 3 m deep sill from the rest of Lake Lucerne. It is well known for its persistent basin-scale deep water seiching of several centimeters per second amplitude with a period of more than 8 h

Table 1. Reactions Included in the Model Study

Reaction Number	Stoichiometry	Scenario Used			
		1	2	3	4
R1	$(CH_2O) + O_2 \rightarrow CO_2 + H_2O$	x	x	x	x
R2	$5/4\ (CH_2O) + NO_3^- + H^+ \rightarrow 1/2\ N_2 + 5/4\ CO_2 + 7/4\ H_2O$			x	
R3	$1/2\ CH_4 + O_2 \rightarrow 1/2\ CO_2 + H_2O$		x		
R4	$2\ Mn^{2+} + O_2 + 2\ H_2O \rightarrow 2\ MnO_2 + 4\ H^+$		x		
R5	$4\ Fe^{2+} + O_2 + 10\ H_2O \rightarrow 4\ Fe(OH)_3 + 8\ H^+$		x		
R6	$1/2\ CH_2O + NO_3^- \rightarrow 1/2\ NO_2^- + 1/2\ CO_2 + 1/2\ H_2O$				x
R7	$1/2\ CH_2O + NO_2^- + H^+ \rightarrow 1/2\ N_2O + 1/2\ CO_2 + H_2O$				x
R8	$1/2\ CH_2O + N_2O \rightarrow 1/2\ CO_2 + N_2 + 1/2\ H_2O$				x
R9	Built up of enzyme activity				x
R10	Decay of enzyme activity				x

in length [*Gloor et al.*, 1994] resulting from the physical dimensions, stratification, and the regular wind forcing of the system. Normally, inflowing water merges into the surface layer, because the major river input of warm epilimnetic water from an upstream lake. However, the measurements were conducted three weeks after a flood event that discharged warm and highly turbid water into the hypolimnion.

2.2. Data Acquisition

[13] Solute microprofiles were recorded using our lander system LISA which enabled us to record profiles of oxygen and nitrate across the sediment water interface in situ [*Müller et al.*, 2002]. We equipped the lander with amperometric Clarke type oxygen electrodes (Unisense) and potentiometric ion selective electrodes (ISE) for nitrate. Recordings were performed for 90 s at each depth at 3 Hz. The first 60 s were discarded in order to account for the response time of the ISEs (<60 s). The nitrate electrodes were made using 10 μl plastic pipette tips as electrode bodies with an average tip diameter of about 0.6 mm, and membrane solutions were based on tridodecylmethylammonium nitrate [*Wegmann et al.*, 1984] following the procedure described by *Müller et al.* [1998].

[14] The oxygen microelectrodes were calibrated using the signal readings in the water column and in the anoxic part of the sediment. Samples for the oxygen determination by Winkler titration were taken using a Niskin bottle close to the sediment surface every 2 h. Sediment cores were collected and overlying water was measured for nitrate. The potentiometric electrodes were calibrated as described by *Maerki et al.* [2006]. The nitrate concentrations calculated by the Nernst equation $C_{NO3-,Nernst}$ always leveled off at an offset concentration $C_{NO3-,\ off}$ in the sediment. This is due to the non-Nernstian behavior of the electrodes close to the detection limit ($\sim$1 mmol m^{-3}) and the signal increase caused by interfering ions like hydrogen carbonate [*Müller et al.*, 1998]. Therefore, we corrected the data using a two-point calibration. We used the overlying water concentration $C_{NO3-,\ bulk}$, and assumed a concentration of zero at the sediment depth below which the measured nitrate electrode signal remained constant. The corrected concentration was calculated by

$$C_{NO3-,corr} = \frac{C_{NO3-,bulk}}{C_{NO3-,bulk} - C_{NO3-,off}} * C_{NO3-,Nernst}. \qquad (2)$$

Flow velocities were determined using an acoustic doppler velocimeter (Vector, Nortek) that was installed 11 cm above the sediment. In order to monitor the seiching of the bottom boundary layer (BBL), 16 TR-1000 thermistors (RBR Oceanographic Instrumentation) were fixed on the tripod over a 4 m depth range at 25 cm spacing after sensor-to-sensor calibration [*Brand et al.*, 2008] and temperature was logged every 3 s.

[15] Iron, manganese, and methane concentration profiles were measured using a diffusive water sampler with a spatial resolution of 1 cm [*Urban et al.*, 1997] that was inserted into the sediment in the middle of Lake Alpnach over one week in July 2005. Iron was determined photometrically by the phenanthroline method [*Tamura et al.*, 1974] using a Hitachi U-2000 spectrophotometer. Manganese was analyzed using a Metrohm Compact IC 861 ion chromatograph equipped with a Metrosep C 2 100/4.0 column. Methane profiles were also determined using a diffusive water sampler inserted in May 2006. The water samples were analyzed using headspace gas chromatography [*McAullife*, 1971]. We used an Agilent GC with a Carboxen 1010 Plot column (Supelco) and a flame ionization detector.

2.3. Model Setup

2.3.1. Model Structure

[16] For our model study, a simple dynamic diffusion-reaction model following the equation

$$\frac{\partial C_i}{\partial t} = D_i' \frac{\partial^2 C_i}{\partial z^2} + \sum_j \nu_{i,j} R_j, \qquad (3)$$

was used, where C_i is the concentration of the solute i, D'_i stands for the effective diffusion coefficient in the sediment, R_j represents the rate term of reaction j affecting solute i, and $\nu_{i,j}$ is the stochiometric factor of solute i in the reaction j.

[17] The model was implemented using the simulation and data analysis software for aquatic systems, AQUASIM version 2.1e [*Reichert*, 1994, 1998], (see also http://www.aquasim.eawag.ch for topical details on this program). This program contained a sediment compartment and allowed to define any set of state variables and transformation processes and to perform simulations and parameter estimations. In order to solve the partial differential equations numerically, the program discretized the spacial derivatives using a conservative finite difference scheme [*LeVeque*, 1992]. The

Table 2. Reaction Rate Parameterizations Applied in the Model Study

Reaction Number	Rate Law
R1	$R_1 = k_1 \frac{[O_2]}{K_{S\_O2}+[O_2]}$
R2	$R_2 = k_2 \frac{[NO_3^-]}{K_{S\_NO3-}+[NO_3^-]} \frac{K_{I\_NO3-\_O2}}{K_{I\_NO3-\_O2}+[O_2]}$
R3	$R_3 = k_3[O_2][CH_4]$
R4	$R_4 = k_4[O_2][Mn^{2+}]$
R5	$R_5 = k_5[O_2][Fe^{2+}]$
R6	$R_6 = k_6 E \frac{[NO_3^-]}{K_{S\_NO3-}+[NO_3^-]} \frac{K_{I\_NO3-\_O2}}{K_{I\_NO3-\_O2}+[O_2]} \frac{K_{I,NO3-\_NO2}}{K_{I\_NO3-\_NO2}+[NO_2^-]}$
R7	$R_7 = k_7 E \frac{[NO_2^-]}{K_{S\_NO2-}+[NO_2^-]} \frac{K_{I\_NO2-\_O2}}{K_{I\_NO2-\_O2}+[O_2]} \frac{K_{I\_NO2-\_NO2}}{K_{I\_NO2-\_NO2}+[NO_2^-]}$
R8	$R_8 = k_8 E \frac{[N_2O]}{K_{S\_NO2-}+[N_2O]} \frac{K_{I\_N2O\_O2}}{K_{I\_N2O\_O2}+[O_2]} \frac{K_{I\_N2O\_NO2}}{K_{I\_N2O\_NO2}+[NO_2^-]}$
R9	$R_9 = k_9 \left[\frac{[NO_3^-]}{K_{S\_NO3-,E}+[NO_3^-]} \frac{[NO_3^-]}{[NO_2^-]+[NO_3^-]} + \frac{[NO_2^-]}{K_{S\_NO2-,E}+[NO_2^-]} \frac{[NO_2^-]}{[NO_2^-]+[NO_3^-]} \right] \frac{K_{I\_E\_O2}}{K_{I\_E\_O2}+[O_2]} (1-E)$
R10	$R_{10} = -k_{10}E$

procedure guaranteed that discretization errors were not affecting the mass balances which are accurate to machine precision. The spatially discretized partial differential equations were then integrated in time with the algorithm DASSL [*Petzold*, 1983] based on an implicit (backward differencing) variable-step, variable-order GEAR integration technique [*Gear*, 1971]. The routines for parameter estimations minimized the sum of weighted squares of the deviations between model results and measurements and were based on the secant method of *Ralston and Jennrich* [1978].

[18] Four different models with an increasing number of biogeochemical processes were evaluated to investigate the response of aerobic mineralization, RC reoxidation, and denitrification to DBL thickness variations (Table 1). The kinetics of aerobic mineralization and denitrification were formulated as Monod-type rate laws with inhibition terms [*Wang and Van Cappellen*, 1996]. The simplest model described only Monod-type oxygen consumption (scenario 1) and allowed testing whether a single set of Monod Parameters (R1 in Table 2) was sufficient to describe the oxygen profiles recorded under different oxygen regimes in the surface waters.

[19] The interaction between oxygen and RC was modeled as second-order reactions [*Wang and Van Cappellen*, 1996]. Since our study was restricted to the zone of aerobic mineralization and denitrification, no detailed model for methanogenesis, sulfate reduction and reductive dissolution of solid iron and manganese phases was implemented. In a simplified approach, the release of the RC was modeled as sources S_i starting at a certain depth $z_{min,\ i}$ below the sediment (scenario 2):

$$R_{rel,i} = \begin{cases} S_i & if \quad z > z_{\min,i} \\ 0 & if \quad z < z_{\min,i} \end{cases}. \tag{4}$$

The response of denitrification to the variable DBL was analyzed by fitting a Monod-type reaction law for nitrate consumption that was inhibited by oxygen (scenario 3). The potential dynamics of intermediates produced during the denitrification process was calculated with the structured biomass approach (*Wild et al.* [1995], scenario 4).

2.3.2. Implementation of the DBL

[20] The flux of a solute J_i across a DBL is given by

$$J_i = -\beta_i(C_{i,B} - C_{i,S}) = -\frac{D_i}{\delta_{DBL}}(C_{i,B} - C_{i,S}), \tag{5}$$

where β_i is the mass transfer coefficient defined as the ratio between the molecular diffusion coefficient D_i of solute i and the thickness of the DBL. The concentrations $C_{i,B}$ and $C_{i,S}$ refer to the solute in the bulk water and at the sediment surface. The sediment module of AQUASIM allows only the specification of solute concentrations at the upper end of the domain. In order to model the influence of the DBL we included a $\delta_{upper} = 250$ μm thick region above the SWI in the domian. It was assumed that the reaction rates of the considered solutes were negligible above the SWI and therefore molecular diffusion was the only relevant process in this zone. We used $C_{i,B}$ as the upper boundary condition and an observed diffusion coefficient $D_{obs,i}$ was calculated by

$$D_{obs,i} = D_i \frac{\delta_{upper}}{\delta_{DBL}} \tag{6}$$

for the modeled DBL thickness δ_{DBL}. At steady state, the observed diffusion coefficient generated the same flux as would be calculated with variable DBL thickness and the molecular diffusion coefficient.

2.3.3. Boundary and Initial Conditions

[21] In the scenarios 1 and 2 we analyzed the response of mineralization and reoxidation of RC on a changing DBL thickness. Only the DBL thickness was varied and the concentrations of all solutes were kept constant at the upper boundary (oxygen, 150 mmol m^{-3}; iron, manganese, and

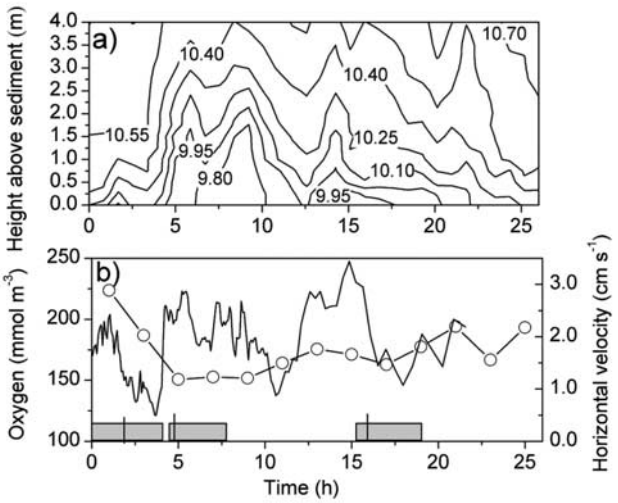

Figure 1. Development of temperature, horizontal flow velocity, and oxygen concentration above the sediment. (a) Isolines of temperature during the 25 h measurement campaign. (b) Horizontal flow velocities (solid line) and oxygen concentrations (circles) measured above the sediment. Grey bars denote the time span during which oxygen and nitrate microprofiles were measured. The vertical line marks the time when the oxygen electrode was right at the sediment water interface (SWI).

methane, 0 mmol m^{-3}). We only calculated the steady state solutions for different thicknesses.

[22] The response of denitrification on a variable DBL was investigated in scenario 3. In a first calculation, we kept the concentrations of nitrate and oxygen constant (nitrate, 16 mmol m^{-3}; oxygen, 150 mmol m^{-3}), and varied the DBL thickness. In order to separate the effects of inhibition and transport limitation on denitrification, we performed additional simulations without a DBL at a fixed nitrate concentration (14.5 mmol m^{-3}) and different oxygen concentrations (from 150 mmol m^{-3} to 42 mmol m^{-3}) at the SWI, which corresponded to the O_2 surface concentrations for different DBL thicknesses.

[23] In scenario 4, we aimed at investigating the complex interplay between microbial processes, production of intermediates during denitrification, transport limitation, and inhibition under changing conditions. In order to calculate a steady state solution, we used the false transient approach. All state variables were initially set to zero. Only the nitrate concentration had an initial value of 1 mmol m^{-3} in order to avoid an infinite reaction rate for the built up of enzymes (R9 in Table 2). We started the simulation with a constant DBL thickness of 0.5 mm until all state variables were constant throughout the profile. This constant solution was independent of the initial conditions. After reaching this time invariant solution, the DBL thickness was forced to oscillate at an amplitude of 0.25 mm. These values for the DBL were comparable to the oscillations of the DBL as observed by *Lorke et al.* [2003] in Lake Alpnach. The upper boundary conditions of all denitrification intermediates were set to 0 mmol m^{-3}, of oxygen to 150 mmol m^{-3} and of nitrate to 16 mmol m^{-3}. In a second simulation run, similar calculations were performed in the absence of a DBL, instead the oxygen concentration at the sediment surface was forced to oscillate between 93 and 133 mmol m^{-3} while keeping all other boundary conditions constant.

3. Results

3.1. Seiching Dynamics and Modeling of Oxygen Profiles

[24] Lake Alpnach demonstrated typical seiching behavior during the field campaign [*Gloor et al.*, 1994; *Brand et al.*, 2008]. The oscillating BBL with the relatively cold interior and a stratified top ascended until t = 10 h and moved slowly back thereafter (Figure 1a). The concentration of oxygen above the sediment (Figure 1b) followed the trend of the temperature, because the well-mixed part of the oscillating BBL was depleted in oxygen compared to the lake interior [see *Brand et al.*, 2008]. The horizontal velocities varied between 0.5 and 3 cm s^{-1}.

3.2. Test of DBL Implementation

[25] We compared our implementation of the DBL using an observed diffusion coefficient with an analytical steady state solution of equation (3) where oxygen consumption follows a first-order rate law with rate constant $k = 20\ h^{-1}$. The analytical expression for the concentration at the sediment surface is

$$C_{i,S} = C_{i,B}\left(1 + \sqrt{kD_i'}\frac{\delta_{DBL}}{D_i}\right)^{-1}. \quad (7)$$

The results of the numeric calculations were in excellent agreement with the analytical model and deviated by less than 1.5% for DBL thicknesses between 0.25 and 2 mm. Therefore, we concluded that our implementation was adequate.

3.3. Dynamics of Mineralization

[26] During the field investigation, three oxygen profiles with different concentrations of oxygen in the water above the sediment were recorded as indicated by the gray bars in Figure 1b. The Monod parameters ($k_1 = 285$ mmol $m^{-3}\ h^{-1}$, $K_{S\_O2} = 4.12$ mmol) for steady state oxic respiration were determined on the basis of scenario 1. The fitted results agreed well with the measured profiles (Figure 2a) and the kinetic parameters were used to assess the influence of a variable thickness of the DBL. In the model, the oxygen concentration at the sediment surface varied between 120 and 50 mmol m^{-3} if the DBL thickness changed from 0.25 mm to 1.5 mm. Simultaneously, the oxygen penetration depth, defined as the depth where the oxygen concentration drops below 10 mmol m^{-3}, decreased from 1.7 mm to 1.2 mm (Figure 2b). The oxygen dynamics were sensitive to changes in the DBL thickness (Figure 3). An increase of the DBL thickness from 0.25 to 1.5 mm diminished the oxygen flux into the sediment from 15 to 9.5 mmol $m^{-2}\ d^{-1}$ which corresponds to a change of more than 30% (Figure 3).

3.4. Dynamics of Dissolved Reduced Compounds

[27] Scenario 2 of the model was designed to study the simultaneous response of reduced compounds and oxygen governed by variable DBL thickness. The source terms and release zones for iron(II), manganese(II) and methane

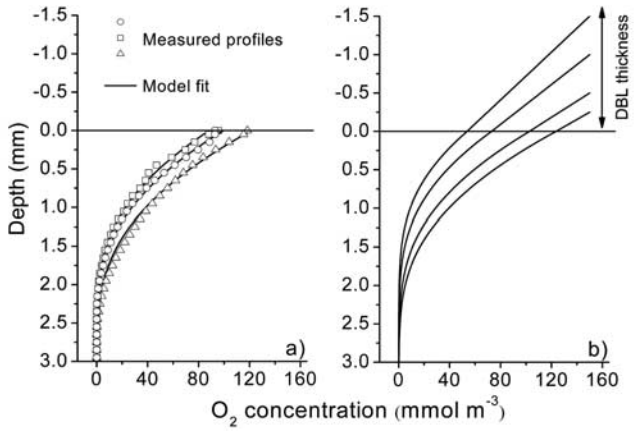

Figure 2. Model results for oxygen dynamics using Monod kinetics. (a) Comparison of fitted (lines) and measured (symbols) data. (b) Calculated oxygen concentrations at variable diffusive boundary layer (DBL) thickness.

(equation (6)) were adjusted in order to reproduce the fluxes toward the sediment obtained from the diffusive water sampler measurements ($S_{Fe} = S_{Mn} = 0.11$ mmol m^{-3} h^{-1}, $S_{CH4} = 1.4$ mmol m^{-3} h^{-1}, $z_{min,Mn} = 20$ mm, $z_{min,Fe} = 30$ mm, $z_{min,CH4} = 20$mm). The model results overestimated the observed concentrations of RC in the deeper part of the sediment. The main cause for this was the omission of reactions that can consume RC like nonequilibrium sorption or mineral precipitation. These secondary processes were omitted in the model in order to focus on the reoxidation of RC close to the SWI. Methane fluxes contributed most to the flux of RC in the sediment ($J_{CH4} = 1.5$ mmol m^{-2} d^{-1}) while iron and manganese fluxes were significantly smaller ($J_{Fe} = 0.1$ mmol m^{-2} d^{-1} and $J_{Mn} = 0.2$ mmol m^{-2} d^{-1}). We used published rate constants for the reoxidation of methane, ferrous iron [*Wang and Van Cappellen*, 1996] and manganese [*Morgan*, 2005]; (see Table 3).

[28] The modeled concentration curves of RC were linear until the solutes diffused into the aerobic zone where they were oxidized (Figures 4a and 4b). Methane was oxidized almost completely in the sediment, whereas about 45% of the Fe(II) and 95% of the Mn(II) were released to the overlying water. The concentration profile of methane was especially sensitive to changes in the DBL thickness. When the DBL thickness was expanded, the lower boundary of the reaction zones for the solutes migrated closer to the sediment surface (Figures 4c and 4d) the surface concentrations of the RC increased (Figure 5a) and their reoxidation rates changed. The influence of the DBL thickness on the methane oxidation was small compared to the Fe and Mn oxidation (Figure 5). The methanotrophic rate slowed down only by 2.5% when the DBL size expanded because CH_4 was almost completely consumed before reaching the sediment-water interface. Iron and manganese oxidation rates showed much higher sensitivity (40 and 80% change) to the DBL thickness since the reaction rate of these compounds was slower and a deeper penetration depth of oxygen increased their residence time in the aerobic zone (Figure 5).

[29] The DBL thickness also controls the proportion of aerobic mineralization and reoxidation. The contribution of RC oxidation to the total sedimentary oxygen flux increased from 22 to 36% when the DBL thickness was raised from 0.25 to 2.0 mm. At the same time, the oxygen flux itself changed from 13 to 8 mmol m^{-2} d^{-1}.

3.5. Influence of Variable DBL Thickness on Denitrifying Processes

[30] Similar to oxygen, nitrate showed a sharp gradient close to the sediment-water interface (Figures 6a and 6b). The measured penetration depth of nitrate was $\approx$ 14 mm and the thickness of the DBL was $\approx$ 0.5 mm during the recording of both profiles. No evidence for nitrification in the aerobic zone of the sediment was found in the nitrate microprofiles. Therefore, we considered only a denitrification rate that was inhibited by oxygen in scenario 3 (Table 2). Even though the difference in the modeled surface concentrations of oxygen was 11 mmol m^{-3} between the recordings at t = 5 and t = 16 h, the calculated nitrate profiles were almost identical and fitted the measurements well. The similarity between the two profiles can be explained by the almost identical DBL during the measurements. Modeled nitrate profiles differed from each other at variable boundary layer thickness (Figure 6c), but a change in the concentration of surface oxygen at constant nitrate produced almost identical profiles (Figure 6d). Still, the smaller oxygen inhibition at lower oxygen concentrations augmented the nitrate flux by 8% (Figure 7). The inset of Figure 6d shows the change of the oxygen gradient in the sediment when less oxygen was present and the denitrification zone moved closer to the sediment surface. The DBL influenced denitrification in two ways: An extended DBL reduced oxygen inhibition and enhanced denitrification but it counterbalanced these effects by imposing a larger transfer resistance for nitrate. As a result, the nitrate flux decreased only by < 5% owing to shifts in DBL thickness (Figure 7).

[31] To investigate the potential behavior of the other nitrogen species nitrite and nitrate, we implemented a sequential denitrification model in scenario 4 that also included the buildup and decay of enzymes catalyzing the denitrification [*Wild et al.*, 1995]. The development of enzyme activity was modeled as a Monod-type process that was limited by the presence of nitrate and nitrite and inhibited by oxygen. The enzyme synthesis would stop at

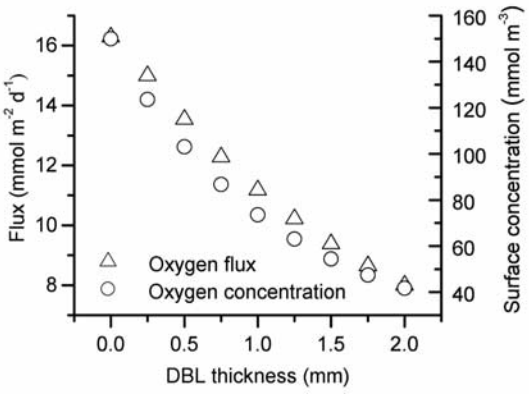

Figure 3. Oxygen flux and oxygen concentrations at the sediment surface as functions of DBL thickness calculated with the Monod model.

Table 3. Transport and Reaction Constants Used in the Model Study

Scenario	Constant	Value	Unit	Source[a]
All	Porosity	0.9		a
All	D_{O2}	5.92×10^{-6}	$m^2\ h^{-1}$	1
3, 4	D_{NO3-}	4.82×10^{-6}	$m^2\ h^{-1}$	1
4	D_{NO2-}	3.71×10^{-6}	$m^2\ h^{-1}$	1
4	D_{N2O}	4.29×10^{-6}	$m^2\ h^{-1}$	1
2	D_{CH4}	4.81×10^{-6}	$m^2\ h^{-1}$	1
2	D_{Fe2+}	1.73×10^{-6}	$m^2\ h^{-1}$	1
2	D_{Mn2+}	1.70×10^{-6}	$m^2\ h^{-1}$	1
1	k_1	285	$mmol\ m^{-3}\ h^{-1}$	f
1	K_{S_O2}	4.12	$mmol\ m^{-3}$	f
2	k_1	197	$mmol\ m^{-3}\ h^{-1}$	f
2	K_{S_O2}	0.1	$mmol\ m^{-3}$	f
2	k_3	2.28	$mmol^{-1}\ m^3\ h^{-1}$	2
2	k_4	0.0006	$mmol^{-1}\ m^3\ h^{-1}$	4
2	k_5	0.004	$mmol^{-1}\ m^3\ h^{-1}$	2
3,4	k_1	285	$mmol\ m^{-3}\ h^{-1}$	f
3,4	K_{S_O2}	0.1	$mmol\ m^{-3}$	f
3	k_2	3.12	$mmol\ m^{-3}\ h^{-1}$	f
3	K_{S_NO3}	3.53	$mmol\ m^{-3}$	f
3	$K_{I\_NO3-\_O2}$	8.74	$mmol\ m^{-3}$	f
4	k_6	3.12	$mmol\ m^{-3}\ h^{-1}$	f
4	K_{S_NO3}	3.98	$mmol\ m^{-3}$	f
4	$K_{I\_NO3-\_O2}$	5.5	$mmol\ m^{-3}$	f
4	$K_{I\_NO3-\_NO2-}$	206.1	$mmol\ m^{-3}$	3
4	k_7	3.12	$mmol\ m^{-3}\ h^{-1}$	3
4	K_{S_NO2-}	38.22	$mmol\ m^{-3}$	3
4	$K_{I\_NO2-\_O2}$	5.69	$mmol\ m^{-3}$	3
4	$K_{I\_NO2-\_NO2-}$	180	$mmol\ m^{-3}$	3
4	k_8	3.12	$mmol\ m^{-3}\ h^{-1}$	3
4	K_{S_N2O}	0.15	$mmol\ m^{-3}$	3
4	$K_{I\_N2O\_O2}$	1.13	$mmol\ m^{-3}$	3
4	$K_{I\_N2O\_NO2-}$	365.5	$mmol\ m^{-3}$	3
4	k_9	1.25	$mmol\ m^{-3}\ h^{-1}$	3
4	$K_{S\_NO3-\_E}$	8.06	$mmol\ m^{-3}$	3
4	$K_{S\_NO2-\_E}$	10.87	$mmol\ m^{-3}$	3
4	$K_{I\_E\_O2}$	3.43	$mmol\ m^{-3}$	3
4	k_{10}	0.16	h^{-1}	3

[a]a, chosen arbitrarily; f, fitted;1, *Boudreau* [1997]; 2, *Wang and Van Cappellen* [1996]; 3, *Wild et al.* [1995]; 4, *Morgan* [2005].

an enzyme activity of 1. However, this value was never reached owing to the continuous decay of enzymes. The model for nitrate reduction was fitted to the measured profiles; for nitrite and nitrous oxide reduction we used the Monod parameters for activated sludge [*Wild et al.*, 1995] owing to the lack of data for sediments. Nevertheless, the calculated values for the nitrous oxide flux using these parameters, $\sim 4.8 \times 10^{-4}$ mmol m^{-2} d^{-1}, were of similar magnitude as the benthic flux of 21.6×10^{-4} mmol m^{-2} d^{-1} determined by *Mengis et al.* [1997] using a mass balance approach in the same lake. The nitrite flux was 0.13 mmol m^{-2} d^{-1}. The variation of both fluxes was less than 1% if the DBL thickness was decreased from 0.25 to 0.75 mm. The modeled nitrite profile showed a maximum concentration of 6 mmol m^{-3} at $\sim$10 mm depth and a penetration of more than 60 mm (Figure 8), the concentration of nitrous oxide in the sediment reached around 11 μmol m^{-3} with a slightly higher penetration depth than nitrite. Maximum enzyme activity was found around 3 mm, right below the zone where no oxygen was available and nitrate concentrations were around 6.5 mmol m^{-3}. The peak concentrations of nitrite and nitrous oxide were far below the zone of oxygen depletion at around 6.5 and 6.8 mm. The local maximum of nitrous oxide at 2 mm was due to the relatively high sensitivity of the nitrous oxide reduction to the presence of oxygen in comparison with the sensitivity of its production from nitrite.

3.6. Effects of the Oscillating DBL

[32] The dynamics of Lake Alpnach are mainly driven by internal seiching and the resulting variability of the DBL. Two scenarios were designed to investigate the influence of this dynamic condition. In the first scenario, we applied a sinusoidal DBL thickness varying between 0.25 and 0.75 mm at different periods (T) from 0.5 to 24 h. In a second scenario we varied only the corresponding surface concentration of oxygen by 113 ± 19 mmol m^{-3} (mean ± amplitude). At T < 6 h, the relative amplitude (the ratio between the absolute amplitude and the average value over a full oscillation period) of the fluxes of all solutes was highly sensitive to the variation frequency of the DBL thickness. It increased from 45 to 62% at T = 0.5 h to 20% at T = 6 h (Figure 9a). The relative amplitude for the oxygen flux remained constant at T > 6 h, whereas nitrogen species' fluxes dropped below 10% for T > 24 h. In contrast, a decrease of the amplitude of solute fluxes was observed when only the surface oxygen concentration was changed. In this case, oxygen fluxes varied over 350% of their average and even oxygen fluxes out of the sediment were observed during times when oxygen concentrations were decreasing at the sediment surface. Nevertheless, the fluxes of the nitrogen species varied only up to 7% of their average (Figure 9b). The decrease of the amplitude of nitrite and nitrate was linked to the smaller variability of the O_2 penetration depth at lower frequencies. Only nitrous oxide showed a slight maximum at T = 3 h. Even though the fluxes of all species varied significantly during an oscilla-

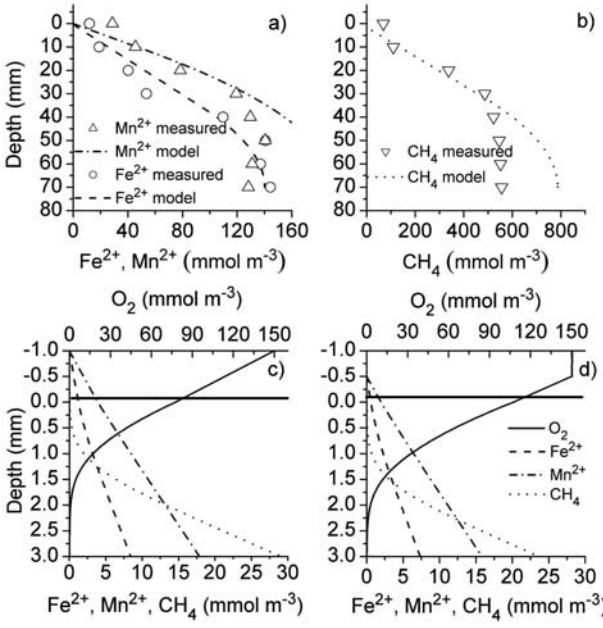

Figure 4. Measured and fitted concentration profiles of (a) manganese and iron and (b) methane. Detailed modeled depth profile of these solutes and oxygen in the aerobic zone at a DBL thickness of (c) 1.0 mm and (d) 0.5 mm.

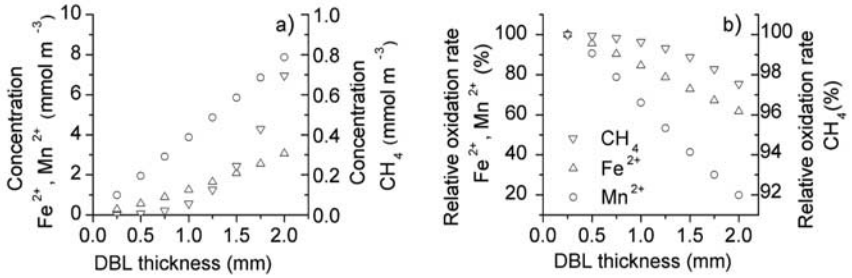

Figure 5. (a) Concentrations of manganese, iron, and methane at the SWI. (b) Relative oxidation rate of the reduced compounds in the aerobic zone of the sediment as a function of the DBL thickness (100% corresponds to the oxidation rate at a DBL thickness of 0.25 mm).

tion period, the influence of the transient variability of the DBL thickness or the oxygen surface concentration on the average fluxes was less than 1% for all solutes.

4. Discussion

[33] The main purpose of our model study was to investigate the short-term effects of variable near-sediment flow velocities and oscillating DBL on the solute dynamics in the uppermost sediment. The model results allow us to address the research questions presented in the introduction.

4.1. Response of Mineralization Dynamics

[34] To explore the response of oxygen fluxes to changes in the DBL, we initially attempted to identify zones in the sediment with different zero-order reaction rates using the method of *Berg et al.* [1998]. At least two reaction zones with lower rates at greater depth were necessary to fit the profiles adequately. The inadequacy of the zeroth-order model for the description of sediment oxygen profiles has been reported previously for other measurement sites [*Epping and Helder*, 1997]. The lower oxygen consumption rate in the deeper parts of the sediment also contrasted the increasing reaction rates in the lower part of the oxic zone as they were observed in many marine systems [*Jørgensen and Boudreau*, 2001; *Rasmussen and Jørgensen*, 1992]. Usually such fast reaction rates were induced by the reoxidation of highly reactive RC in marine systems [*Glud et al.*, 2007]. However, these pathways played a less important role in Lake Alpnach, where a higher OM loading resulted in a smaller contribution of RC reoxidation (<40%) to the sediment oxygen demand.

[35] In order to describe the different profiles under variable conditions, the zeroth-order reaction rates had to be varied by more than 30% in each zone. By contrast, all three profiles could be modeled with a single set of Monod parameters by only varying the oxygen concentration at the sediment surface. The Monod model for oxygen consump-

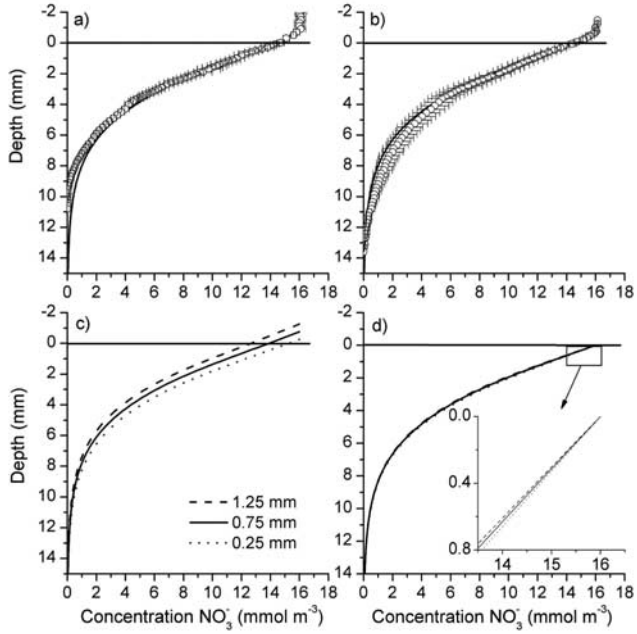

Figure 6. Comparison between measured (dots) and fitted (line) nitrate profiles at (a) 5 h and (b) 16 h. The measured DBL thickness was 0.5 mm in both cases. The error bars denote the standard deviations between several electrodes and reflect the spatial heterogeneity. (c) Modeled nitrate profiles at three different DBL thicknesses. (d) Modeled nitrate profiles at oxygen concentrations that correspond to the surface concentrations at the three DBL extensions.

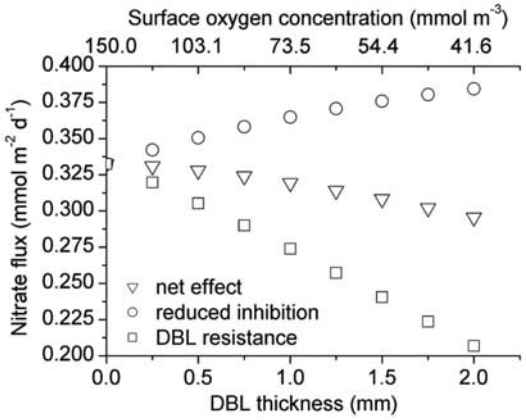

Figure 7. Influence of the DBL on nitrate reduction in Lake Alpnach. Circles denote the increase of the nitrate flux by oxygen inhibition; squares denote the reduction due to DBL resistance; and triangles denote the overall decrease of the nitrate flux due to increasing DBL thickness. Note that the corresponding surface oxygen concentration intervals shown on the upper axis are not equidistant.

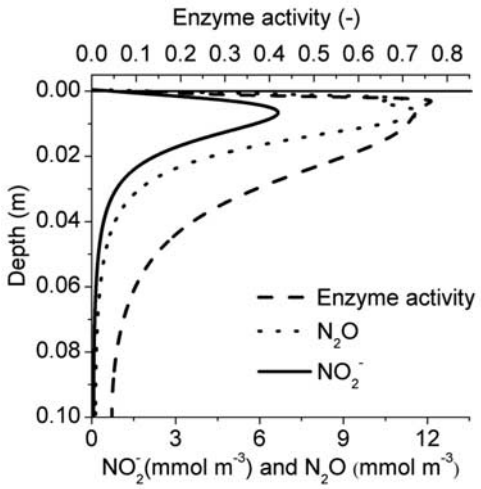

Figure 8. Steady state profiles of nitrite, nitrous oxide, and enzyme activity calculated with scenario 4 at a DBL thickness of 0.5 mm.

tion was therefore more applicable under dynamic conditions and was used in the further scenarios.

[36] The calculated response of oxygen flux in the sediment (change > 30%) to DBL dynamics was similar to the 25% reduction calculated for Aarhus Bay during late autumn [*Glud et al.*, 2007] and to the 22% change for highly reactive organic carbon [*Kelly-Gerreyn et al.*, 2005]. This comparison indicates that the DBL plays an important role in the oxygen dynamics of mesotrophic lakes where the settled organic material is still highly reactive. An even higher sensitivity of oxygen fluxes to DBL changes could be expected in sediments of eutrophic lakes if enough oxygen is present and if it is mainly consumed via mineralization of organic matter.

[37] Oxygen consumption via different pathways is critical in this context. *Jørgensen and Boudreau* [2001] showed in a theoretical model that the sensitivity of the oxygen flux to the DBL thickness can be strongly damped if the oxygen demand is mainly caused by reduced dissolved compounds. Our calculations for Lake Alpnach show a significant decrease of oxygen flux with increasing DBL thickness even if aerobic reoxidation of RC was included in the model. The proportion of RC to the sediment oxygen flux of less than 40% was apparently too low to act as a "buffer" against DBL dynamics. The fraction of O_2 consumed by RC should be quite variable among different lakes. A recent microsensor study in eutrophic Lake Zug indicated that about 50% of the oxygen flux was consumed by reoxidation of RC [*Maerki et al.*, 2009].

4.2. Mechanisms and Extent of DBL Control on Other Solutes Fluxes

[38] The DBL mainly acts as a resistance to mass transfer at the sediment-water interface. Consequently, the modeled fluxes of the solutes diffusing into the sediment, like oxygen and nitrate, showed the highest sensitivity toward a change of the diffusion distance caused by a variable DBL. This sensitivity decreased with the distance of the reactive zone from the sediment surface and with slower reaction rates. In the model, the oxygen flux decreased by 47% when a 2 mm thick DBL was imposed, whereas the nitrate flux was reduced by only 11%. The influence of the DBL on dissolved RC like methane, manganese and ferrous iron was twofold. The DBL did not only act as a diffusion resistance, it also controlled the penetration depth and flux of oxygen into the sediment. This affected the oxidation of these compounds by defining the location and extent of the reaction zone for RC. As a consequence, expanding the DBL shifted the portion of oxygen flux by RC from 22 to 36% while the oxidation of RC changed only from 2.9 mmol m^{-2} d^{-1} to 2.8 mmol m^{-2} d^{-1}. Similar results were obtained by *Glud et al.* [2007] in their study of Aarhus Bay where the contribution of RC to the sedimentary oxygen uptake was over 70%.

[39] Our calculations showed that the DBL decreased the nitrate uptake in the sediment by imposing a diffusion resistance. This is in contrast with the findings of *Kelly-Gerreyn et al.* [2005] who observed a decreasing nitrate release with increasing DBL thickness from the sediments in most of their model runs. They observed nitrate uptake only for highly reactive organic carbon. The main reason for this discrepancy was the omission of nitrification in our model since the available data allowed us to exclude this process in the top millimeters of Lake Alpnach sediments.

[40] *O'Connor and Hondzo* [2008b] performed studies in a laboratory flume on denitrification under variable flow conditions. They found that nitrate removal increased with flow velocity under moderate flow conditions that were similar to those in lake Alpnach (u_* below 0.23 cm s^{-1}).

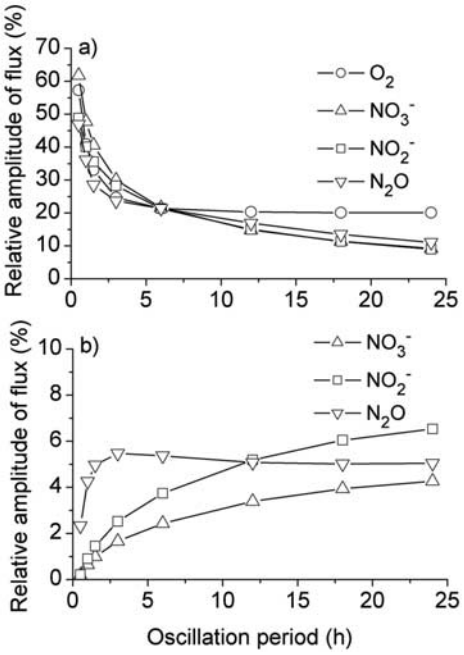

Figure 9. Relative amplitude of solute fluxes (defined as the ratio between flux amplitudes and average flux over a full oscillation cycle) at different period lengths. (a) Results obtained when an oscillating DBL thickness is imposed; (b) results obtained for oscillating oxygen concentrations at the SWI.

Nevertheless, they observed a decrease of denitrification rates at higher flow velocities that was only partly explained by the increased diffusion length of nitrate. They argued that the zone of denitrification was forced into regions where the abundance of denitrifying bacteria as well as the availability of labile organic carbon may be lower. We do not expect such limiting effects in our system, since denitrification was observed down to one cm in the sediment and such a deep oxygen penetration depth is quite unlikely in lake Alpnach. Similar observations like those reported from *O'Connor and Hondzo* [2008b] were also reported by *Arnon et al.* [2007]. In their experiment, they observed a decrease in denitrification in a biofilm at high flow velocities (5 cm s^{-1}). The whole biofilm was aerobic under these conditions. They explained the decreasing denitrification by metabolic shifts of facultative denitrifiers. The structured biomass approach, as adapted from *Wild et al.* [1995], includes such a metabolic shift by considering the enzyme activity. The implementation of more complex denitrification models that include growth and decay of biomass could provide additional insights if calibrated with specific data of the microbial communities involved.

[41] Results from scenario 4, which evaluated denitrification intermediates, suggested that the inhibition effect of oxygen as controlled by the DBL was negligible under steady state conditions. However, this indirect effect via inhibition became more important under dynamic conditions with time scales of less than one day.

4.3. Implications of Seiching Induced Variability

[42] In the dynamic model, the fluxes averaged over the full seiching period deviated by less than 1% from the steady state solutions. This negligible deviation also confirmed the validity of our conclusions drawn from the steady state calculations in the previous scenarios if time scales of more than one period are considered. However, instantaneous deviations from steady state profiles can be higher than 20% for oxygen and 10% for other nitrogen species for oscillation periods in Lake Alpnach which are shorter than 24 h [*Münnich et al.*, 1992]. Such large short-term variations have been reported by *Lorke et al.* [2003] who observed variable oxygen fluxes between 6 and 13.2 mmol m^2 d^{-1} during a 24 h campaign in Lake Alpnach. This result indicates that single profiles recorded in the upper few mm of the sediments must be interpreted carefully if the solutes are highly sensitive to DBL variations and the investigated system is highly dynamic. In this case, microprofiles can only represent the state of the sediment at a certain time interval.

[43] These dynamics of seiching systems may also be critical for the recording of the profiles. Since oxygen profiles are most sensitive to variations in DBL thickness and oxygen concentrations, it is quite critical to record them under constant conditions. In our study, we needed approximately 40 min to record the oxygen profiles. This time span was small compared to the seiching dynamics of the lake. In contrast, 180 min were necessary to record the nitrate profiles. Our model study showed that changes of the DBL thickness and oxygen concentrations had only a minor effect on the nitrate profiles in the deeper regions of the sediment. It is quite likely that spatial variability masks the temporal variation of such nitrate profiles.

[44] The combination of noninvasive flux measurements (eddy correlation technique) which integrate over larger areas at high temporal resolution [*Brand et al.*, 2008; *McGinnis et al.*, 2008] with profiling at high spatial resolution in the sediment can improve the understanding of these highly dynamic mineralization and reoxidation processes. The eddy correlation method seems to be a promising tool for flux measurements that integrate over a certain surface area [*Berg et al.*, 2007].

[45] By contrast, mineralization processes that occur several centimeters below the aerobic zone like methanogenesis or reductive iron dissolution appear to be mainly unaffected by DBL dynamics. This decoupling of processes in anoxic sediment layers simplifies both the measurement and interpretation of gradients and diffusive fluxes of reduced compounds below the aerobic zone.

4.4. Relevance of Other Phenomena at the Sediment Water Interface

[46] While our study focused on DBL variations on a time scale of typical seiching motions, *Røy et al.* [2004] and *Gundersen and Jørgensen* [1990] observed short-term fluctuations at time scales below 50 s. We performed simulations that considered such high-frequency fluctuations and found that they had no significant influence on the average oxygen and nitrate fluxes (<2%) and were limited to sediment depths of less than 0.3 mm. *O'Connor and Hondzo* [2008a] found that periodic displacements of water parcels due to sweep and eject motions also contributed to the solute transfer at the sediment water interface. Nevertheless, their findings mainly affected the way of how to quantify the time averaged solute transfer coefficient and the effective DBL thickness (compare equation (4)). Since the typical time scale of these eddies was shorter than 1 s, the penetration depth of these fluctuations into the sediment was negligible. The simplifying concept of a variable DBL thickness therefore still represents a valid model for studying the effects of changing solute transfer at time scales of minutes and hours.

[47] Several studies have shown that advective flow could occur in some types of sediments. This flow is induced by shear [*Svensson and Rahm*, 1991] and leads to a significant enhancement of solute transport by dispersion [*Güss*, 1998]. Also Darcy flow is observed if pressure gradients exist. These gradients can be caused by the flow field on mounds and ripples [*Huettel et al.*, 1998] as well as by surface waves [*Webb and Theodor*, 1968]. These advective phenomena are mainly observed in sandy sediments with a high permeability. Sediments of deep lakes such as Lake Alpnach consist of silty mud with a generally low permeability [*Boudreau*, 2001] and, therefore, we do not expect any pressure driven flows in the sediment. In addition, the typical amplitude of the seiching at the surface ($\sim$10 cm) was too small to induce a significant pressure gradient.

[48] Another factor that may influence solute dynamics is the surface structure of the sediment [*Røy et al.*, 2002] since it defines the area, at which the exchange occurs. The underestimation of the flux induced by ignoring the three-dimensional structure is around 10–30% depending on the sediment topography. Still, the error decreases with increasing DBL thickness, since the DBL smoothes out rough elements. In Lake Alpnach, we find a typical DBL thickness

between 0.2 and 0.9 mm and therefore ignoring the topography will result in only a minor error.

5. Conclusion

[49] Our model study has shown that the DBL is an important factor for the control of solute dynamics in the first millimeters in the sediment of seiche driven lakes. The developed model enabled us to investigate the dynamics of potential processes at temporal and spatial scales which are beyond the capabilities of present measurement techniques. It also allowed us to integrate the tight coupling of biogeochemical and physical processes and to highlight the importance of temporal dynamics induced by seiching.

[50] **Acknowledgments.** We thank Michael Schurter, Daniela Richter, and Torsten Diem for the support in the field. Daniel McGinnis and David Senn kindly improved the English. We are grateful to Peter Reichert for developing the sediment module of AQUASIM and his great support during this work.

References

Archer, D., S. Emerson, and C. R. Smith (1989), Direct measurement of the diffusive sublayer at the deep-sea floor using oxygen microelectrodes, *Nature*, *340*, 623–626, doi:10.1038/340623a0.

Arnon, S., K. A. Gray, and A. I. Packman (2007), Biophysicochemical process coupling controls nitrate use by benthic biofilms, *Limnol. Oceanogr.*, *52*, 1665–1671.

Baumann, B., M. Snozzi, J. R. Van der Meer, and A. J. B. Zehnder (1997), Development of stable denitrifying cultures during repeated aerobic-anaerobic transient periods, *Water Res.*, *31*, 1947–1954, doi:10.1016/S0043-1354(97)00053-5.

Berg, P., N. Risgaard-Petersen, and S. Rysgaard (1998), Interpretation of measured concentration profiles in sediment pore water, *Limnol. Oceanogr.*, *43*, 1500–1510.

Berg, P., H. Røy, and P. L. Wiberg (2007), Eddy correlation flux measurements: The sediment surface area that contributes to the flux, *Limnol. Oceanogr.*, *52*, 1672–1684.

Boudreau, B. P. (1997), *Diagenetic Models and Their Implementation*, Springer, Berlin.

Boudreau, B. P. (2001), Solute transport above the sediment water interface, in *The Benthic Boundary Layer*, edited by B. P. Boudreau and B. B. Jørgensen, pp. 4–43, Oxford Univ. Press, New York.

Boudreau, B. P., and N. L. J. Guinasso (1982), The influence of a diffusive sublayer on accretion, dissolution, and diagenesis at the sea floor, in *The Dynamic Environment at the Ocean Floor*, edited by K. A. Fanning and F. T. Manheim, pp. 115–145, Lexington, Lexington, Mass.

Brand, A., D. F. McGinnis, B. Wehrli, and A. Wüest (2008), Intermittency of oxygen flux into the bottom boundary of lakes as observed by eddy correlation, *Limnol. Oceanogr.*, *53*, 1997–2006.

Epping, E. A. G., and W. Helder (1997), Oxygen budgets calculated from in situ oxygen microprofiles for northern Adriatic sediments, *Cont. Shelf Res.*, *17*(14), 1737–1764, doi:10.1016/S0278-4343(97)00039-3.

Gear, C. W. (1971), The automatic integration of ordinary differential equations, *Commun. ACM*, *14*(3), 176–179, doi:10.1145/362566.362571.

Gloor, M., A. Wüest, and M. Münnich (1994), Benthic boundary mixing and resuspension induced by internal seiches, *Hydrobiologia*, *284*, 59–68, doi:10.1007/BF00005731.

Glud, R. N., P. Berg, H. Fossing, and B. B. Jørgensen (2007), Effect of the diffusive boundary layer on benthic mineralization and O_2 distribution: A theoretical model analysis, *Limnol. Oceanogr.*, *52*, 547–557.

Gundersen, J. K., and B. B. Jørgensen (1990), Microstructure of diffusive boundary layers and the oxygen uptake of the sea floor, *Nature*, *345*, 604–607, doi:10.1038/345604a0.

Güss, S. (1998), Oxygen uptake at the sediment-water interface simultaneously measured using a flux chamber method and microelectrodes: Must a diffusive boundary layer exist?, *Estuarine Coastal Shelf Sci.*, *46*(1), 143–156.

Höhener, P., and R. Gächter (1994), Nitrogen cycling across the sediment-water interface in an eutrophic, artificially oxygenated lake, *Aquat. Sci.*, *56*, 115–132, doi:10.1007/BF00877203.

Hondzo, M., T. Feyaerts, R. Donovan, and B. L. O'Connor (2005), Universal scaling of dissolved oxygen distribution at the sediment-water interface: A power law, *Limnol. Oceanogr.*, *50*, 1667–1676.

Huettel, M., W. Ziebis, S. Forster, and G. W. Luther III (1998), Advective transport affecting metal and nutrient distributions and interfacial fluxes in permeable sediments, *Geochim. Cosmochim. Acta*, *62*, 613–631, doi:10.1016/S0016-7037(97)00371-2.

Jørgensen, B. B., and B. P. Boudreau (2001), Diagenesis and sediment-water exchange, in *The Benthic Boundary Layer*, edited by B. P. Boudreau and B. B. Jørgensen, pp. 211–244, Oxford Univ. Press, New York.

Jørgensen, B. B., and D. J. D. Marais (1990), The diffusive boundary-layer of sediments: Oxygen microgradients over a microbial mat, *Limnol. Oceanogr.*, *35*, 1343–1355.

Jørgensen, B. B., and N. P. Revsbech (1985), Diffusive boundary-layers and the oxygen-uptake of sediments and detritus, *Limnol. Oceanogr.*, *30*, 111–122.

Kelly-Gerreyn, B. A., D. J. Hydes, and J. J. Waniek (2005), Control of the diffusive boundary layer on benthic fluxes: A model study, *Mar. Ecol. Prog. Ser.*, *292*, 61–74, doi:10.3354/meps292061.

LeVeque, R. J. (1992), *Numerical Methods for Conservation Laws*, Birkhäuser, Boston.

Lorke, A., L. Umlauf, T. Jonas, and A. Wüest (2002), Dynamics of turbulence in low speed oscillating bottom-boundary layers of stratified basins, *Environ. Fluid Mech.*, *2*, 291–313, doi:10.1023/A:1020450729821.

Lorke, A., B. Müller, M. Maerki, and A. Wüest (2003), Breathing sediments: The control of diffusive transport across the sediment-water interface by periodic boundary layer turbulence, *Limnol. Oceanogr.*, *48*, 2077–2085.

Maerki, M., B. Müller, and B. Wehrli (2006), Microscale mineralization pathways in surface sediments: A chemical sensor study in Lake Baikal, *Limnol. Oceanogr.*, *51*, 1342–1354.

Maerki, M., B. Müller, C. Dinkel, and B. Wehrli (2009), Pathways of organic matter mineralization in lake sediments with different oxygen and organic carbon supply, *Limnol. Oceanogr.*, in press.

McAullife, C. (1971), GC determination of solutes by multiple phase equilibration, *Chem. Technol.*, *1*, 46–51.

McGinnis, D. F., P. Berg, A. Brand, C. Lorrai, T. J. Edmonds, and A. Wüest (2008), Measurements of eddy correlation oxygen fluxes in shallow freshwaters: Towards routine applications and analysis, *Geophys. Res. Lett.*, *35*, L04403, doi:10.1029/2007GL032747.

Mengis, M., R. Gächter, and B. Wehrli (1997), Sources and sinks of nitrous oxide (N_2O) in deep lakes, *Biogeochemistry*, *38*, 281–301, doi:10.1023/A:1005814020322.

Morgan, J. J. (2005), Kinetics of reaction between O_2 and Mn (II) species in aqueous solutions, *Geochim. Cosmochim. Acta*, *69*, 35–58, doi:10.1016/j.gca.2004.06.013.

Müller, B., K. Buis, R. Stierli, and B. Wehrli (1998), High spatial resolution measurements in lake sediments with PVC based liquid membrane ion-selective electrodes, *Limnol. Oceanogr.*, *43*, 1728–1733.

Müller, B., M. Märki, C. Dinkel, R. Stierli, and B. Wehrli (2002), In situ measurements in lake sediments using ion-selective electrodes with a profiling lander system, in *Environmental Electrochemistry: Analyses of Trace Element Biogeochemistry*, edited by M. Taillefert and T. F. Rozan, pp. 126–143, Am. Chem. Soc., Washington, D. C.

Münnich, M., A. Wüest, and D. M. Imboden (1992), Observations of the 2nd vertical-mode of the internal seiche in an alpine lake, *Limnol. Oceanogr.*, *37*, 1705–1719.

O'Connor, B. L., and M. Hondzo (2008a), Dissolved oxygen transfer to sediments by sweep and eject motions in aquatic environments, *Limnol. Oceanogr.*, *53*, 566–578.

O'Connor, B. L., and M. Hondzo (2008b), Enhancement and inhibition of denitrification by fluid-flow and dissolved oxygen flux to stream sediments, *Environ. Sci. Technol.*, *42*, 119–125, doi:10.1021/es071173s.

Petzold, L. (1983), A description of DASSL: A differential/algebraicsystem solver, in *Scientific Computing: Applications of Mathematics and Computing to the Physical Sciences*, edited by R. S. Stepleman, pp. 65–68, North-Holland, Amsterdam.

Ralston, M. L., and R. I. Jennrich (1978), DUD: A derivative-free algorithm for nonlinear least squares, *Technometrics*, *20*(1), 7–14, doi:10.2307/1268154.

Rasmussen, H., and B. B. Jørgensen (1992), Microelectrode studies of seasonal oxygen-uptake in a coastal sediment: Role of molecular-diffusion, *Mar. Ecol. Prog. Ser.*, *81*, 289–303, doi:10.3354/meps081289.

Reichert, P. (1994), Aquasim: A tool for simulation and data-analysis of aquatic systems, *Water Sci. Technol.*, *30*, 21–30.

Reichert, P. (1998), *AQUASIM 2.0 — User Manual: Computer Program for the Identification and Simulation of Aquatic Systems*, Swiss Fed. Inst. for Environ. Sci. and Technol., Dubendorf, Switzerland.

Røy, H., M. Huettel, and B. B. Jørgensen (2002), The role of small-scale sediment topography for oxygen flux across the diffusive boundary layer, *Limnol. Oceanogr.*, *47*, 837–847.

Røy, H., M. Huettel, and B. B. Jørgensen (2004), Transmission of oxygen concentration fluctuations through the diffusive boundary layer overlying aquatic sediments, *Limnol. Oceanogr.*, *49*, 686–692.

Santschi, P., P. Bower, U. P. Nyffeler, A. Azevedo, and W. S. Broecker (1983), Estimates of the resistance to chemical transport posed by the deep sea boundary layer, *Limnol. Oceanogr.*, *28*, 899–912.

Steinberger, N., and M. Hondzo (1999), Diffusional mass transfer at sediment-water interface, *J. Environ. Eng.*, *125*, 192–200, doi:10.1061/(ASCE)0733-9372(1999)125:2(192).

Svensson, U., and L. Rahm (1991), Toward a mathematical model of oxygen transfer to and within bottom sediments, *J. Geophys. Res.*, *96*, 2777–2783, doi:10.1029/90JC02209.

Tamura, H., K. Goto, T. Yotsuyanagi, and M. Nagayama (1974), Spectrophotometric determination of iron (II) with 1,10–phenanthroline in the presence of large amounts of iron (III), *Talanta*, *21*, 314–318, doi:10.1016/0039-9140(74)80012-3.

Urban, N. R., C. Dinkel, and B. Wehrli (1997), Solute transfer across the sediment surface of a eutrophic lake. 1. Porewater profiles from dialysis samplers, *Aquat. Sci.*, *59*, 1–25, doi:10.1007/BF02522546.

Wang, Y. F., and P. Van Cappellen (1996), A multicomponent reactive transport model of early diagenesis: Application to redox cycling in coastal marine sediments, *Geochim. Cosmochim. Acta*, *60*, 2993–3014, doi:10.1016/0016-7037(96)00140-8.

Webb, J. E., and J. Theodor (1968), Irrigation of submerged marine sands through wave action, *Nature*, *220*, 682–683, doi:10.1038/220682a0.

Wegmann, D., H. Weiss, D. Ammann, W. E. Morf, E. Pretsch, K. Sugahara, and W. Simon (1984), Anion-selective liquid membrane electrodes based on lipophilic quarternary ammonium compounds, *Microchim. Acta*, *84*, 1–16, doi:10.1007/BF01204153.

Wild, D., R. Vonschulthess, and W. Gujer (1995), Structured modeling of denitrification intermediates, *Water Sci. Technol.*, *31*, 45–54, doi:10.1016/0273-1223(95)00179-Q.

A. Brand, Department of Civil and Environmental Engineering, University of California, 205 O'Brien Hall, Berkeley, CA 94720, USA. (andreas_brand@berkeley.edu)

C. Dinkel and B. Wehrli, Surface Waters Research and Management, Eawag, Seestrasse 79, CH-6047 Kastanienbaum, Switzerland.